30 June 2000

ELSEVIER

Chemical Physics Letters 324 (2000) 149–155

CHEMICAL PHYSICS LETTERS

www.elsevier.nl/locate/cplett

Potential energy landscape for proton transfer in $(H_2O)_3H^+$: comparison of density functional theory and wavefunction-based methods

Phillip L. Geissler [a,*], Troy Van Voorhis [a], Christoph Dellago [a,b]

[a] *Department of Chemistry, University of California, Berkeley, CA 94720, USA*
[b] *Department of Chemistry, University of Rochester, Rochester, NY 14627, USA*

Received 13 April 2000

Abstract

Predictions of the BLYP density functional are compared with wavefunction-based calculations for several structural and dynamical properties of $(H_2O)_3H^+$. We focus attention on properties important for proton transfer in this cluster. Good agreement between density functional theory (DFT) calculations and all-electron MP2 results is found for energies, structures, and vibrational properties of both transition states and stable states. Good agreement between DFT and MP2 results is also observed for the potential experienced by the transferring proton in the transition state region. Structural predictions of empirical models compare well with the ab initio results.

1. Introduction

In order to study the dynamics of proton transfer in complex systems of chemical and biological interest, it is necessary to adopt approximate methods for computing the energies and forces involved. Considerable discussion has been devoted recently to the accuracy of such methods, most notably electron density functional theory (DFT). The simplest system for which proton transfer properties can be compared, the protonated water dimer, has been studied thoroughly [1,2]. In its equilibrium state, the excess proton is shared evenly between the two water molecules, so that proton transfer does not occur naturally as an activated process. A barrier to transfer in this cluster exists only when the distance between oxygen nuclei is constrained to values greater than those observed at equilibrium. The widely used BLYP density functional significantly underestimates the heights of such barriers. The accuracy of the BLYP functional for proton transfer reactions in general is therefore questionable. The quality of approximate methods is more difficult to evaluate, however, when they are applied to bulk systems in which proton transfer occurs naturally. Geissler et al. have examined a system of intermediate complexity, the protonated water trimer $(H_2O)_3H^+$, using DFT as well as an empirical model [4,5]. This cluster is sufficiently complex that proton transfer is an activated process involving reorganization of the cluster as a whole. The system is simple

* Corresponding author. E-mail: geissler@gold.cchem.berkeley.edu

0009-2614/00/$ - see front matter
PII: S0009-2614(00)00479-6

enough, however, that its collective motions may be visualized easily and its energetics may be computed accurately.

In the present Letter, we examine in detail the suitability of DFT for studying proton transfer in $(H_2O)_3H^+$. Using wavefunction-based methods, we analyze the equilibrium state and transition states for this process. Optimized geometries, energetics, and vibrational properties are presented in Section 2. Predictions of the BLYP functional are shown to agree almost quantitatively. We discuss a more stringent test of the dynamics generated by BLYP in Section 3. Specifically, we determine BLYP and MP2 forces and energies at a number of configurations along a reactive trajectory computed from BLYP forces. Small differences in equilibrium bond distances account for the largest discrepancies, and overall qualitative agreement is good. Some insight into the observed agreement between density functional and MP2 theories is gained by studying the effective potential in which the transferring proton moves as the system passes through the transition state. This potential, discussed in Section 4, exhibits a single minimum, indicating that the activation barrier arises from collective reorganization rather than bond dissociation. The large errors in bond dissociation barriers predicted by BLYP in the case of constrained $H_5O_2^+$ are not relevant for proton transfer in this larger cluster.

2. Stable states and transition states

In the minimum energy state of the protonated water trimer, a well-defined hydronium ion H_3O^+ donates hydrogen bonds to two terminal water molecules. This asymmetry of oxygen atoms allows for isomerization processes in which the excess proton is transferred from one water molecule to another. (We number the donating and accepting molecules 1 and 2, respectively. See Fig. 1.) In Refs. [4,5] the structures most important for isomerization were identified by analyzing ensembles of proton transfer trajectories generated by a simple empirical model and by DFT. In order for proton transfer to occur, it was found, molecule 3 must move across the cluster and accept a hydrogen bond from molecule 2. From the transition state configurations shown in Fig. 1b,c the system may relax with the excess proton bound to either molecule 1 or molecule 2. In the present work we study these stable state and transition state structures in detail using different levels of electronic structure calculation. In each case we have determined these structures by energy minimization, using either molecular dynamics or conjugate gradient optimization. For transition states minimization was performed subject to symmetry constraints which characterize the saddle points [5]. We have confirmed that all identified transition states possess a single unstable normal mode.

As a benchmark, we have performed wavefunction-based calculations. Energies and optimized geometries of the minimum and two transition states were obtained with second order Møller–Plesset perturbation theory (MP2) in a TZP basis [6,7] using Q-CHEM [8]. To evaluate the accuracy of this approach, we computed the activation energies for these transition states with larger basis sets and a higher degree of correlation using ACES II [9]. MP2/cc-pVTZ//MP2/TZP [10] and MP2/cc-pVQZ//MP2/TZP [10] results for each stationary point were used to estimate the complete basis set (CBS) limit using standard techniques [11,12]. (Here, MP2/cc-pVTZ//MP2/TZP denotes a MP2/cc-pVTZ calculation performed with the MP2/TZP geometry.) The importance of additional correlation was incorporated using CCSD(T)/cc-pVTZ//MP2/TZP results. Assuming that this additional correlation is additive [13,14], we estimate the CCSD(T)/CBS energies. Because the MP2/TZP activation energies agree with the estimated CCSD(T)/CBS values to within 0.5 kcal/mol (see Table 1), we use the former, simpler method for subsequent wavefunction-based calculations.

We compare these wavefunction-based results to predictions of DFT. For all DFT calculations we used CPMD [15] with the gradient-corrected BLYP functional [16,17] and Martins–Troullier pseudopotentials [18] with a plane-wave cutoff of 70 Ry. A box length of 11.11 Å and cluster boundary conditions were applied [19]. Optimizations of nuclear geometries were performed by dynamic annealing in which momenta were quenched periodically. The geometries of the energy minimum and relevant saddle points obtained using DFT agree well with

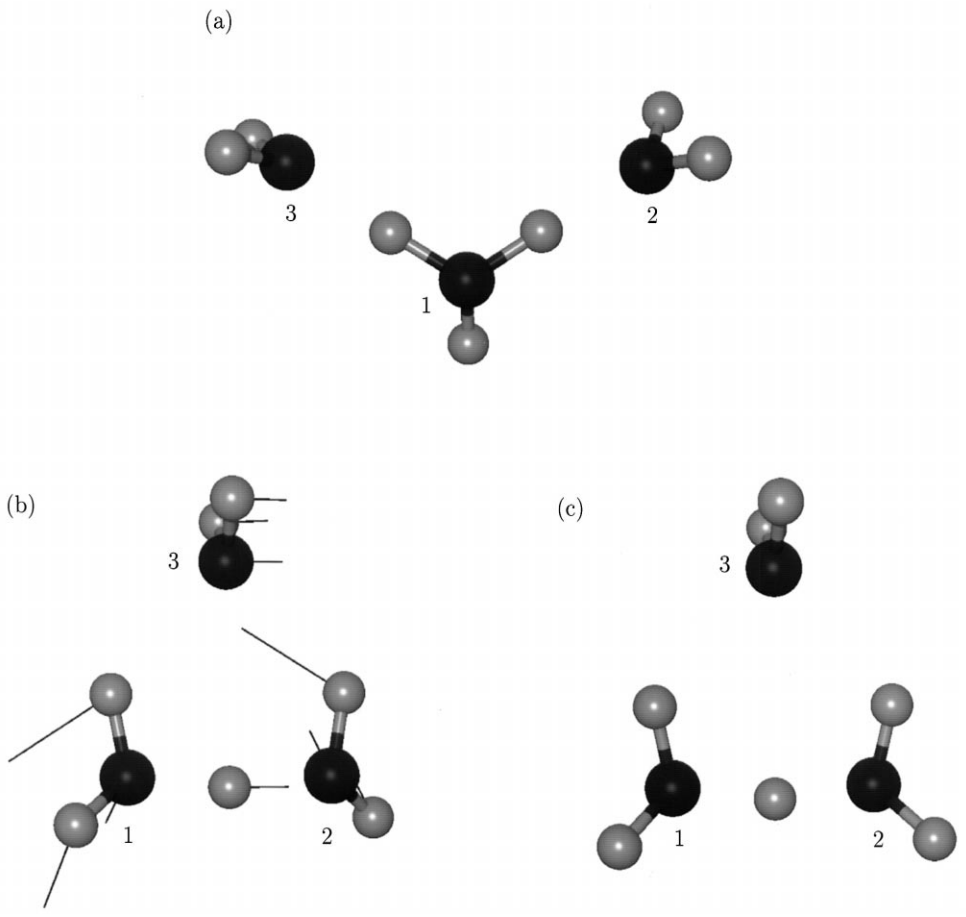

Fig. 1. Potential energy minimum (a) and saddle points (b) and (c) for proton transfer determined using MP2 energies. In the stable state (a) a hydronium ion is associated with molecule 1. Water molecules 2 and 3 accept hydrogen bonds from the ion. In order to reach a transition state, molecule 3 must move across the cluster and form a hydrogen bond with molecule 2. In (b) lines originating at atomic centers indicate the directions and relative magnitudes of atomic motions in the unstable mode.

MP2 results. The resulting MP2 structures are depicted in Fig. 1. Bond distances, oxygen ring angles, and molecular orientations of the transition states predicted by BLYP all lie within a few percent of the corresponding MP2 results. The determined stable states differ only by small rotations of the terminal water molecules about their hydrogen bonds to the central hydronium ion.

Remarkably, simple empirical models predict stable state and transition state geometries that are similar to those determined by ab initio methods. For example, the stable state and transition state structures obtained using the Stillinger–David model [20] of polarizable and dissociable water (see Ref. [4]) agree qualitatively with those in Fig. 1. We have also analyzed the multi-state empirical valence bond (MS-EVB) model of Schmitt and Voth as applied to this cluster. In the MS-EVB model a list of diabatic states must be defined for any given configuration. To describe the stable states we use three coupled diabatic states. In each of the three diabatic states, a different oxygen atom is bound to the excess proton. For the transition states we use a four state description. Two of these diabatic states describe binding of the excess proton to molecules 1 and 2. In the two remaining states, molecule 3 is identified as the

hydronium ion, so that charge may effectively delocalize throughout the cluster. Although this MS-EVB model was parameterized to reproduce equilibrium properties of small protonated water clusters [3], the structures of transition states in $(H_2O)_3H^+$ agree well with MP2 results. Bond lengths and angles differ by only a few percent.

Activation energies of the two transition states for proton transfer are given in Table 1. Agreement among MP2, CCSD(T), and BLYP is excellent for both barrier heights. These results also agree well with the recent DFT calculations by Wales [21]. The simple empirical models described above predict barrier heights that are several kcal/mol larger.

The C_2-symmetric transition state (Fig. 1b), in which water dipoles at the base of the oxygen triangle are anti-parallel, lies only 0.8 kcal/mol lower in energy than the C_s symmetric structure, (Fig. 1c), in which the alignment is parallel. Vibrational analysis of these saddle point regions (discussed below) suggests that their entropies are comparable. Consequently, both transition states should contribute to proton transfer dynamics at room temperature. Using canonical transition state theory with MP2 energies and vibrational frequencies, we estimate a branching ratio of 2 at ambient conditions.

An analysis of the potential energy surface in the vicinity of these structures provides information regarding transition dynamics. By diagonalizing the mass-weighted Hessian matrix, we have computed vibrational spectra and eigenmodes of the stable state and lower- energy transition state. The spectra are plotted in Fig. 2. BLYP results differ most from MP2 results (~ 200 cm^{-1}) for high frequencies corresponding to O–H stretches. For slower, collective motions BLYP and MP2 frequencies differ by less than 70 cm^{-1}. A comparison of vibrational modes is similarly favorable. The direction of the unstable mode is depicted in Fig. 1b. It is mainly comprised of an oxygen ring distortion which destroys the symmetry of water molecules 1 and 2. We estimate the error in the corresponding BLYP result through the scalar product of vectors η^{MP2} and η^{BLYP}, whose elements are the components of the normalized modes. For the unstable mode, $\eta^{\mathrm{MP2}} \cdot \eta^{\mathrm{BLYP}} = 0.99$, i.e. the orientations of these

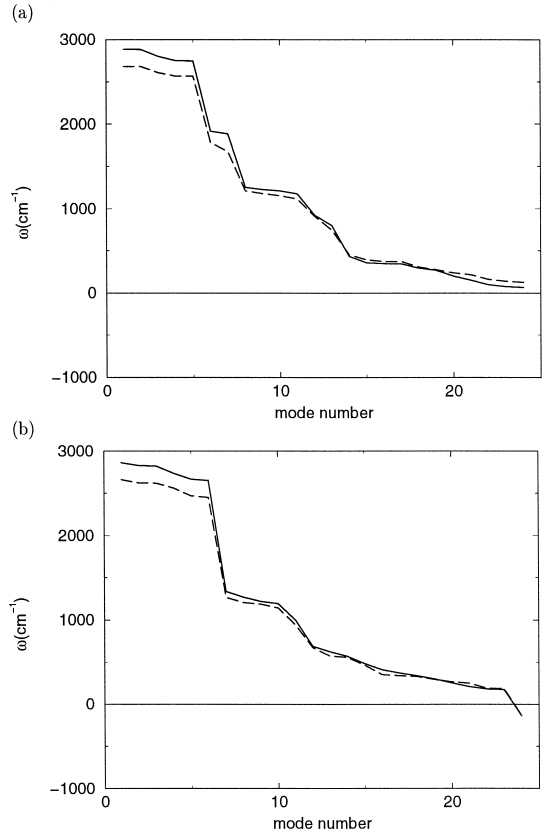

Fig. 2. Vibrational frequencies ω of (a) the potential energy minimum and (b) the lower energy transition state for BLYP (dashed line) and MP2 (solid line) calculations. The frequency of the unstable mode at the transition state is plotted as the negative of its magnitude. As in our previous work, we assign a mass of 2 amu to all hydrogen atoms.

Table 1
Energies ΔE_1 and ΔE_2 of the transition states shown in Fig. 1b,c, respectively, obtained by various methods. Energies are reported relative to the potential energy minimum. The first two rows show results of wavefunction-based calculations. The last three rows show the results of the BLYP density functional, the Stillinger–David model, and an empirical valence bond model, respectively.

Method	ΔE_1 (kcal/mol)	ΔE_2 (kcal/mol)
MP2/TZP	5.8	6.7
CCSD(T)/CBS	5.4	6.2
DFT/BLYP	5.7	6.4
Stillinger–David	11.7	14.2
MS-EVB	9.6	10.6

modes agree within 1%. Differences of only a few percent are observed for other transition state modes.

3. Trajectory analysis

The agreement between BLYP and MP2 predictions of minima, saddle points, and local curvature of the $(H_2O)_3H^+$ potential energy surface suggests that forces evaluated by DFT may be used to compute dynamics reliably. As a more demanding test, we have used MP2 calculations to examine a proton transfer trajectory generated by BLYP forces. The trajectory we consider is taken from Ref. [5]. It begins at the lower-energy transition state and has initial momenta which excite the unstable mode. Nuclear positions were advanced from these initial conditions for 150 fs using Car–Parrinello molecular dynamics [22]. In this time, the cluster relaxes from the transition state and, at 75 fs, passes near the potential energy minimum in Fig. 1a. Inertia carries the system past the minimum, and potential energy increases as the hydrogen bond between molecule 3 and the newly formed hydronium ion is strained. Energy profiles along this path are plotted in Fig. 3. BLYP and MP2 energies and forces deviate as the hydronium ion is formed around time $t \approx 75$ fs. The largest energetic differences, ~ 2 kcal/mol, can be reduced significantly (though not fully) by relaxing the position of the transferring proton on the MP2 energy surface, while holding all other nuclear degrees of freedom fixed. This relaxation process moves the proton less than 0.1 Å, suggesting that errors in configurations along the trajectory are principally intramolecular and are not large.

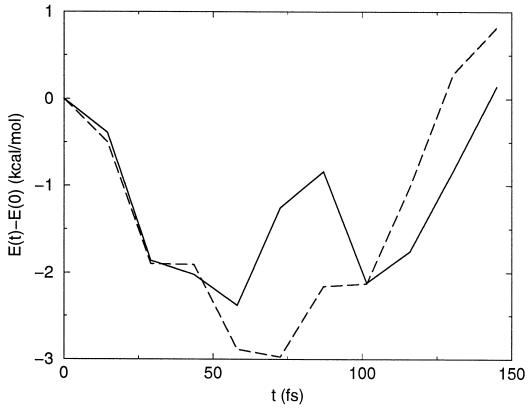

Fig. 3. Energy $E(t)$ of configurations along a BLYP proton transfer trajectory as a function of time t. The dashed line denotes BLYP results. The solid line shows energies of these configurations as determined by MP2 theory.

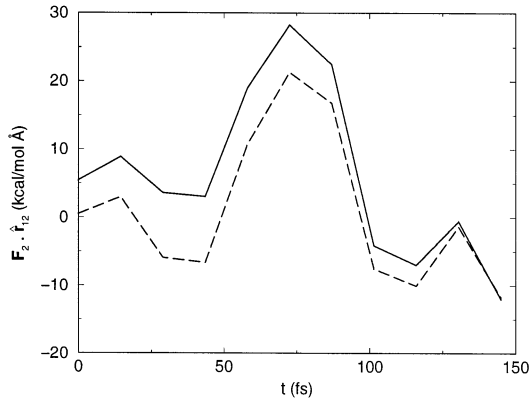

Fig. 4. Force $\boldsymbol{F}_2$ on oxygen atom 2, projected onto the O_1–O_2 axis, as a function of time t along the same BLYP trajectory as in Fig. 3. The dashed line again represents BLYP results, while the solid line represents MP2 results.

Gradients of the potential energy allow an even more detailed analysis of this trajectory. For a simple comparison, we have projected nuclear forces onto the line connecting oxygen atoms 1 and 2, described by the unit vector $\hat{\boldsymbol{r}}_{12}$. Motion of the unstable mode occurs primarily in the direction of this vector. The forces experienced by oxygen 2 during the transfer are the largest in the cluster and are plotted in Fig. 4. A comparison of these BLYP forces to MP2 gradients is representative. Qualitative trends over the course of the trajectory agree well, but significant differences of ~ 10 kcal/mol Å are observed. Relaxation of the transferring proton again suggests that these large discrepancies arise from intramolecular energetics that are sensitive to small nuclear displacements.

4. Potential of the transferring proton

As a final comparison between density functional theory and MP2 calculations, we consider the instantaneous potential experienced by the transferring pro-

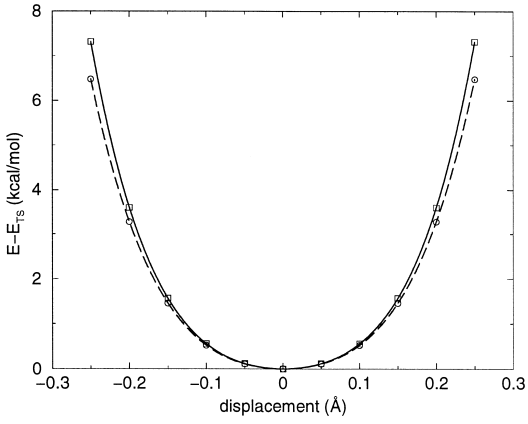

Fig. 5. Energy as a function of excess proton displacement at the lower energy transition state. Displacement is performed parallel to the O_1–O_2 line. BLYP calculations are shown as circles connected by a dashed line. MP2 calculations are shown as squares connected by a solid line.

ton at the transition state. We project the potential onto a single dimension by measuring the energy required to displace the proton along the line of transfer, i.e. parallel to $\hat{\boldsymbol{r}}_{12}$. This potential is plotted as a function of proton displacement in Fig. 5. BLYP and MP2 results differ only slightly for displacements up to 0.25 Å. In both cases a single minimum centered between the donating and accepting water molecules is observed. The shape of the instantaneous potential reflects the mechanism of proton transfer and has implications for the expected importance of proton tunneling. From the normal mode analysis in Section 2, it is clear that the reaction coordinate is dominated by cluster rearrangement rather than simple bond dissociation. As this collective reaction coordinate progresses, the minimum of the instantaneous proton potential shifts towards the accepting water molecule, and the proton is transferred. In this respect proton transfer in $(H_2O)_3H^+$ is quite different from transfer in $H_5O_2^+$ with oxygen centers constrained at separations larger than the equilibrium value. In the latter system, the constraint requires that the excess proton cross a barrier due to bond dissociation in order for proton transfer to occur. For the protonated water trimer it is instead the energetics of cluster reorganization, or effective solvation, that are responsible for the barrier to proton transfer. Because the coordinate describing this reorganization has a large associated mass, significant kinetic effects due to tunneling are not expected.

Acknowledgements

P.L.G. is a National Science Foundation Predoctoral Fellow and was a Berkeley Fellow for part of this work. T.V. is a National Science Foundation Predoctoral Fellow. In its initial stages this research was supported by the Director, Office of Science, Office of Basic Energy Sciences, of the US Department of Energy under Contract No. DE-AC03-76SF00098. It was completed with support for P.L.G. and C.D. from DOE Grant DE-FG03-99ER14987. Some of the calculations in this work were performed on a RS/6000 SP provided through an IBM SUR grant.

References

[1] S. Sadhukhan, D. Muñoz, C. Adamo, G.E. Scuseria, Chem. Phys. Lett. 306 (1999) 83.
[2] M.E. Tuckerman, D. Marx, M.L. Klein, M. Parrinello, Science 275 (1997) 817.
[3] U.W. Schmitt, G.A. Voth, J. Chem. Phys. 111 (1999) 9361.
[4] P.L. Geissler, C. Dellago, D. Chandler, Phys. Chem. Chem. Phys. 1 (1999) 1317.
[5] P.L. Geissler, C. Dellago, D. Chandler, J. Hutter, M. Parrinello, Chem. Phys. Lett. 321 (2000) 225.
[6] S. Huzinaga, J. Chem. Phys. 42 (1965) 1293.
[7] T.H. Dunning, J. Chem. Phys. 55 (1971) 716.
[8] C.A. White et al., Q-CHEM, Version 1.2., Q-Chem, Inc., Pittsburgh, PA, 1998.
[9] J.F. Stanton, J. Gauss, W.J. Lauderdale, J.D. Watts, R.J. Bartlett, ACES II. The package also contains modified versions of the MOLECULE Gaussian integral program of J. Almlöf, P.R. Taylor, the ABACUS integral derivative program written by T.U. Helgaker, H.J.A. Jensen, P. Jørgensen, P.R. Taylor, and the PROPS property evaluation integral code of P.R. Taylor.
[10] T.H. Dunning, J. Chem. Phys. 90 (1989) 1007.
[11] J.M.L. Martin, Chem. Phys. Lett. 259 (1996) 669.
[12] W. Kuzelnigg, J.D. Morgan, J. Chem. Phys. 96 (1992) 4484.
[13] L.A. Curtiss et al., J. Chem. Phys. 94 (1991) 7221.
[14] L.A. Curtiss et al., J. Chem. Phys. 110 (1999) 4703.
[15] J. Hutter, A. Alavi, T. Deutsch, M. Bernasconi, St. Goedecker, D. Marx, M. Tuckerman, M. Parrinello, CPMD,

MPI für Festkörperforschung and IBM Zurich Research Laboratory, 1995–1999.
[16] A.D. Becke, Phys. Rev. A 38 (1988) 3098.
[17] C. Lee, W. Yang, R.G. Parr, Phys. Rev. B 37 (1988) 785.
[18] N. Troullier, J. Martins, Phys. Rev. B 43 (1991) 1993.
[19] G.J. Martyna, M.E. Tuckerman, J. Chem. Phys. 110 (1999) 2810.
[20] F.H. Stillinger, C.W. David, J. Chem. Phys. 69 (1978) 1473.
[21] D.J. Wales, J. Chem. Phys. 111 (1999) 8429.
[22] R. Car, M. Parrinello, Phys. Rev. Lett. 55 (1985) 2471.